Cellular Physiology and Biochemistry

Cell Physiol Biochem 2018;50:512-524
DOI: 10.1159/000494165
Published online: 11 October 2018
Accepted: 2 October 2018

Original Paper

miR-136-5p Regulates the Inflammatory Response by Targeting the IKKβ/NF-κB / A20 Pathway After Spinal Cord Injury

Guiying Deng[a,b,d] Yunbing Gao[b] Zhongxi Cen[b] Jichen He[b] Baichuan Cao[b] Gaofeng Zeng[c] Shaohui Zong[b,d]

[a]Research Centre for Regenerative Medicine and Guangxi Key Laboratory of Regenerative Medicine, Collaborative Innovation Center of Guangxi Biological Medicine, Guangxi Medical University, Nanning, [b]Department of Spine Osteopathia, the First Affiliated Hospital of Guangxi Medical University, Nanning, [c]College of Public Hygiene of Guangxi Medical University, Nanning, [d]Research Center for Regenerative Medicine, Guangxi Medical University, Nanning, China

Key Words
Spinal cord injury • Inflammation • miR-136-5p • Viral transfection • IKKβ/NF-κB/A20

Abstract
Background/Aims: miR-136-5p participates in recovery after spinal cord injury (SCI) via an unknown mechanism. We investigated the mechanism underlying the involvement of miR-136-5p in the inflammatory response in a rat model of SCI. ***Methods:*** Sprague-Dawley rat astrocytes were cultured *in vitro* to construct a reporter plasmid. Luciferase assays were used to detect the ability of miR-136-5p to target the IKKβ and A20 genes. Next, recombinant lentiviral vectors were constructed, which either overexpressed miR-136-5p or inhibited its expression. The influence of miR-136-5p overexpression and miR-136-5p silencing on inflammation was observed *in vivo* in an SCI rat model. The expression of IL-1β, IL-6, TNF-α, IFN-α, and related proteins (A20, IKKβ, and NF-κB) was detected. ***Results:*** *In vitro* studies showed that luciferase activity was significantly activated in the presence of the 3′ untranslated region (UTR) region of the IKKβ gene after stimulation of cells with miR-136-5p. However, luciferase activity was significantly inhibited in the presence of the 3′UTR region of the A20 gene. Thus, miR-136-5p may act directly on the 3′UTR regions of the IKKβ and A20 genes to regulate their expression. miR-136-5p overexpression promoted the production of related cytokines and NF-κB in SCI rats and inhibited the expression of A20 protein. ***Conclusion:*** Overexpression of miR-136-5p promotes the generation of IL-1β, IL-6, TNF-α, IFN-α, IKKβ, and NF-κB in SCI rats but inhibits the expression of A20. Under these conditions, inflammatory cell infiltration into the rat spinal cord increases and injury is significantly aggravated. Silencing of miR-136-5p significantly reduces the protein expression results described after miR-136-5p overexpression and ameliorates the inflammatory cell infiltration and damage to the spinal cord. Therefore, miR-136-5p might be a new target for the treatment of SCI.

Y. Gao and Z. Cen contributed equally to this work.

Shaohui Zong
and Gaofeng Zeng

Dept Spine Osteopathia, the First Affliated Hospital of Guangxi Medical University
No.6 Shuangyong Road, Nanning, Guangxi (China)
Tel. +86-0771-5358959, E-Mail xiaohui3008@126.com

Introduction

Spinal cord injury (SCI) is a common and frequently occurring clinical condition that usually affects young adults. The clinical manifestations are associated with high morbidity and high mortality [1]. SCI not only causes severe physical and psychological damage to the patient, but also represents a considerable economic burden to society [2]. The main treatment methods for SCI currently include drug therapy, surgical treatment, and transplantation therapy. These treatments aim to reduce secondary injury and promote nerve recovery and regeneration [3-5]. However, no SCI treatment can achieve a complete cure or exert significant curative effects in the clinic.

The major pathological changes associated with SCI include neuronal and glial necrosis and apoptosis. These changes are not conducive to the repair and treatment of the damaged tissue and the SCI site is affected by inflammation caused by inflammatory cells and the generation of inflammatory factors. Excessive immune inflammation also accelerates neuronal necrosis and axonal demyelination [6, 7].

NF-κB is a transcription factor found in almost all types of eukaryotic cell. In spinal cord tissue, NF-κB is mainly present in nerve cells, astrocytes, oligodendrocytes, and microglia [8]. IKK is a complex that contains many types of protein components and that promotes the activation of key kinases. IKKα and IKKβ show high homology, and both proteins are present in the IKK complex. In the resting state, NF-κB binds to its inhibitory monomer (IκB) [9]. The protein remains in the cytoplasm at rest but is activated by SCI in nerve cells, glial cells, and vascular endothelial cells [10-12]. Activated NF-κB enters the nucleus and binds to the κB sequence in the promoter or enhancer of the target gene to promote the expression of a large number of inflammatory cytokines, inflammatory chemokines, and adhesion molecules that target gene release, such as IL-1, TNF-α, IL-6, IL-8, and ICAM-1. Activated cytokines can enhance the expression of NF-κB, further boosting the release of cytokines such as TNF-α, IL-6, and IL-1, forming a cascade amplification effect that aggravates secondary damage after SCI [13-15]. A20 is an important regulator of NF-κB that negatively regulates the anti-apoptotic action of NF-κB. A20 is also involved in the changes in immune responses and autoimmune diseases that occur in many pathophysiological processes associated with inflammation and the immune system [16, 17]. A20-deficient rats are likely to have chronic inflammation and inflammatory damage to multiple organs and are extremely sensitive to TNF-α [18]. These results indicate that A20 is an ideal target molecule that slows down the inflammatory response.

The expression and post-transcriptional regulation of many genes play an important role after SCI [7, 19, 20]. MicroRNAs (miRNAs) are important in the development of strategies for regulating spinal cord development and spinal plasticity to promote functional regenerative therapy [21, 22]. miRNAs are endogenous, 20- to 24-nucleotide RNAs. In the human body, miRNAs depend mainly on the 3' untranslated region (UTR) of the target mRNA, which promotes the degradation of the target mRNA or inhibits its translation, thereby regulating gene expression at the transcriptional level and subsequently regulating the function of cells. Therefore, the differential expression of miRNA after SCI may have the potential to regulate gene expression and play an important role in this process [23]. Currently, although increasing evidence shows that miRNAs are involved in the immune response, the available information is insufficient, and there is a lack of detailed studies of specific molecular mechanisms. The regulation of upstream and downstream molecules and the signaling pathways involved must be thoroughly studied to reveal the regulation of the miRNA regulatory network after SCI. Therefore, in this study, a rat model of SCI was established and miR-136-5p was studied *in vitro* and *in vivo*. Our work will increase our understanding of miR-136-5p regulation after SCI and promote the development of therapeutic measures for SCI.

Materials and Methods

Ethics statement

This project met the standards of the ethics review committee and considered and protected the rights and interests of the research participants. The study was approved by the Medical Ethics Committee of the First Affiliated Hospital of Guangxi Medical University.

Materials

Fetal bovine serum (FBS) and Dulbecco's modified Eagle's medium (DMEM)/F12 were purchased from HyClone (Logan, UT, USA). Trypsin was purchased from Sigma-Aldrich (St. Louis, MO, USA). A20 and NF-κB antibodies were purchased from Abcam (Cambridge, MA, USA); β-actin rabbit polyclonal antibody was purchased from Bioss Inc. (Guangzhou, China). Astrocytes were isolated from the cerebral cortex of 2-day-old Sprague-Dawley rats (Experimental Animal Center of Guangxi Medical University).

Extraction, culture, and identification of rat astrocytes

Rat hippocampal astrocytes were cultured according to the McCarthy method [24]. One-day-old newborn Sprague-Dawley rats were soaked in 75% ethanol for 3 to 5 min after disinfection of the skin and decapitated. The skull was carefully cut and removed under sterile conditions, and the blood vessels and meninges were separated. The hippocampus was cut into small pieces and digested with 0.125% trypsin for 30 min. Digestion was stopped with liquid DMEM/F12 containing 10% FBS. The cells were gently pipetted and centrifuged at 1200 rpm for 5 min. Next, the cells were filtered through a stainless steel mesh (ϕ = 200 μm) and transferred to a glass culture flask that was coated with poly-L-lysine hydrobromide. The appropriate amount of complete DMEM/F12 was then added. The cell suspension was gently and repeatedly triturated, the cell density was adjusted to 1.0×10^6/ml, and the cells were differentially attached at 37°C in a 5% CO_2 incubator for 30–60 min to remove fibroblast components. The cell suspension was transferred to a polylysine-coated flask and cultured at 37°C in a 5% CO_2 incubator. The medium was replaced every 2 to 3 days. Cell growth was observed under a microscope confluency reached 90% (on day 7). After incubation of the cultures with shaking at 240 rpm for 24 h at 37°C, the supernatant was discarded. To obtain adequately purified astrocytes, the above steps were performed once again at an interval of 1–2 days. The cell medium was discarded and the cells were digested with 0.125% trypsin and transferred to 24-well plates precoated with polylysine. The plating density was 1.0×10^6 cells/cm^2. The cells were incubated for 4–5 days at 37°C in a 5% CO_2 incubator, and GFAP staining was performed. Staining was observed under a fluorescence microscope, and the presence of positive staining and no background staining was verified.

Construction of dual-luciferase reporter plasmids and transfection of Sprague-Dawley rat astrocytes

RayBiotech (Guangzhou, China) synthesized genes containing the IKKβ-WT 3'UTR (containing approximately 100 bp upstream and downstream of the entire predicted miR-136-5p binding sequence) and the IKKβ-mutant 3'UTR (compared with the IKKβ-WT 3'UTR, this construct is missing the entire predicted miR-136-5p binding sequence). Genes containing the A20-WT 3'UTR (containing 100 bp fragments upstream and downstream of the entire predicted miR-136-5p binding sequence) and the A20-mutant 3'UTR (compared with the A20-WT 3'UTR, this construct is missing the entire predicted miR-136-5p binding sequence) were also synthesized. XhoI and NotI restriction sites were located on both ends of the plasmid; the psiCHECK-2 multiple cloning site of the dual-luciferase reporter plasmid was then recombined to obtain the wild-type and mutant clones, and the accuracy of the constructs was confirmed by sequencing.

Rat hippocampal astrocytes were seeded in 96-well plates at 5×10^3 cells per well, cultured in DMEM for 24 h, and washed twice with antibiotic-free DMEM; transfection reagents were prepared according to Lipofectamine 2000 instructions. Then, 0.2 μg of the dual-luciferase reporter plasmid and a 20 nmol/l final concentration of the miR-136-5p mimic (RayBiotech) or the negative control were co-transfected into rat hippocampal astrocytes, and the medium was replaced with complete DMEM after 6 h. Luciferase activity was detected 48 h later using the Dual-Luciferase Reporter Assay System (Promega, Madison, WI, USA).

Construction and clinical evaluation of a rat SCI model

Forty-eight Sprague-Dawley rats were randomly divided into four groups with 12 rats in each group. The Sham group was sham-operated. In each group (Sham, SCI+LV-ctrl, SCI+LV-miR136-5p, and SCI+LV-sponge), 3 rats were sacrificed on day 1, 3 were sacrificed on day 3, and the remainder were sacrificed on day 7.

Each Sprague-Dawley rat was given an intraperitoneal injection of 0.3 ml of 10% chloral hydrate per 100 g. After the anesthesia took effect, the rats were fixed in the prone position and routinely disinfected with a towel to determine the position of the T10 spinous process; then, the skin of the surgery field was subjected to povidone-iodine disinfection. A 3-cm skin incision was made, the subcutaneous fascia was separated, the paraspinal muscles were bluntly separated along the edge of the spinous process with haemostatic forceps, the spinous processes were exposed, and ophthalmologic scissors were used to cut the spinous and interspinous ligaments, fully exposing the T9–T11 spinous processes. Preserving the T9 spinous process, we pinched off the T10 spinous process, exposed the T10 lamina, gently removed the ligamentum flavum between the T9 and T10 lamina, and squeezed the forceps to pinch the T10 lamina and expose the dura mater. A self-made improved Allen's device was used, in which a 10 g Kirschner wire free falls from a height of 3 cm and hits the dural sac, resulting in an impact injury to the T10 segment of the spinal cord. After the impact, the injured spinal cord was disinfected with warm water, and the muscles, fascia, and skin were sutured in order. The SCI model was considered a success when, upon impact of the Allen's device against the spinal cord, the rat's body vibrated, both lower limbs rapidly retracted and rebounded, and the tail tilted. As soon as the device fell, it hit the surface of the spinal cord and rapid bleeding occurred. In the Sham group, the lamina was exposed but the rats were not subjected to damage treatment.

After surgery, the rats were maintained in individual cages and subcutaneously injected with 300, 000 units of penicillin, once per day for 3 days. Bladder compression urination was recorded twice daily. The BBB (Basso, Beattie, and Bresnahan) scoring method [12] (21 levels) was used as a functional assessment to evaluate behavior and hindlimb motor function in the rats before and after SCI. The evaluations were performed before injury and on postoperative days 1, 3, and 7, and each index was measured three times. The BBB scores were determined by researchers who were not aware of the experimental group but were familiar with the scoring criteria. All animals were examined before the evaluation. The degree of bladder filling affects the activity of the bladder.

Lentiviral vector (miR-136-5p) Construction and transfection in a rat model of SCI

Lentiviral vector construction, packaging, and titer determination were performed by Guangzhou Yijin Biotechnology Co., Ltd., and the constructs were verified by sequencing. Each experimental group was injected with the corresponding lentiviral suspension (2×10^8 TU per rat, 200 μl) through the tail vein on day 7 before surgery and on the day of surgery. In the Sham group, the same volume of sterile saline was injected. The day after surgery was counted as day 0 in the SCI group. In each group (SCI+LV-ctrl, SCI+LV-miR136-5p, and SCI+LV-sponge), 3 rats were sacrificed on day 1, 3 were sacrificed on day 3, and the remainder were sacrificed on day 7.

Postoperative animal behavior observation and scoring

Behavioral observations were performed using the mouse scale for locomotion (BMS) score proposed by Basso et al. [25]. The scores were mainly determined by observing mouse hindlimb joint activity, foot toe contact, and trunk stability after SCI. The rating levels range from 0 to 9. A score of 0 indicates that the hindlimb motor function is completely impaired, whereas 9 indicates that the mouse hindlimb exercise function is completely normal. The mice were adapted to exercise for 20 min on an open countertop every day for 3 days before the experiment. After the SCI, two non-experimenters familiar with the BMS score independently observed the rats at 20:00 each night to blindly score the mouse hindlimb locomotor function. The BMS scores were recorded for 1–7 days for each group of mice.

Tissue materials

The animals were anesthetized on day 1, day 3, and day 7 after the operation. Blood was collected from the eyes of the rats and serum was obtained. After the left ventricle was infused with approximately 200 ml of heparin in physiological saline until clear fluid drained, the spinal cord from the SCI site was collected. At the same time point, the spinal cord tissue from the corresponding location in the Sham group was collected.

Double immunofluorescence staining

After lavage with 4% paraformaldehyde, the injured spinal cord tissue and the spinal cord tissue from the Sham group were collected, fixed with 4% paraformaldehyde for 24 h, paraffin-embedded, and serially sectioned. Ten slices were generated with a thickness of 5 μm. First, the paraffin-embedded spinal cord sections were subjected to immunofluorescence staining for NF-κB, IKKβ, and A20. The NF-κB antibody concentrations were 1:100, 1:200, and 1:400. The IKKβ antibody concentrations were 1:100, 1:200, and 1:400. The A20 antibody concentrations were 1:50, 1:100, and 1:200. The sections were stained according to standard immunofluorescence staining conditions and procedures, and the staining results were analyzed to establish the optimal primary antibody concentration. Next, each group of paraffin-embedded spinal cord sections was used for NF-κB, IKKβ, and A20 immunofluorescence staining. According to the determined optimal primary antibody concentration, the spinal cord tissues were subjected to immunofluorescence staining, and the distribution and content of NF-κB, IKKβ, and A20 in the spinal cord tissues were analyzed. Finally, Image-Pro Plus software was used to analyze the images from each group and the optical density values of the NF-κB-, IKKβ-, and A20-positive regions were measured.

Ultrastructural changes in the spinal cord in SCI rats by transmission electron microscopy

The spinal cord tissue was fixed by perfusion with 4% paraformaldehyde. The injured spinal cord tissue and the corresponding spinal cord tissue from the Sham group were removed and placed in 2.5% glutaraldehyde 4°C for 3 h and then cut into 1-mm-thick slices. The slices were placed in 0.1 M bis(arsenate) buffer overnight (4°C). The next day, the samples were fixed in a 1% citric acid solution (pH 7.4) for 90 min. After acetone dehydration, the samples were embedded in EPon 812. Ultrathin sections were mounted on a copper mesh, stained with uranyl acetate and lead tannin, and observed with an H-7650 electron microscope.

Detection of miR-136-5p mRNA expression by real-time PCR

Total RNA was extracted using TRIzol reagent and used to synthesize cDNA with a reverse transcription (RT) kit. According to the manufacturer's protocol, RT-PCR was performed with first-strand cDNA synthesized with 1 μg of total RNA and oligo d(T) 18 primers. The primers for the real-time PCR assays for miR-136-5p were designed using Primer Premier 5.0. β-actin and U6 were used to normalize each sample and each gene. All of the samples were assayed in duplicate.

Enzyme-linked immunosorbent assay for the expression of inflammatory cytokines

Inflammatory cytokine levels (including IL-1β, IL-6, TNF-α, and IFN-α) were determined to examine the effects of miR-136-5p on the levels of cytokines in the injured region. Blood was collected from the eyeball of rats and centrifuged at 1200 rpm to obtain serum. Inflammatory cytokines were detected after 24 h of incubation using a Millipore inflammatory cytokine kit (Millipore, Burlington, MA, USA). The cytokines were incubated with antibodies in enzyme-linked immunosorbent assay (ELISA) plates and, after the plates were washed with additional antibodies, the absorbance was measured using multiple spectra.

Western blot analysis

After harvesting the spinal cord for protein extraction, we determined the protein concentration using a BCA protein assay kit. Western blot analysis was performed using sodium dodecyl sulfate polyacrylamide gel electrophoresis. After the protein was transferred to polyvinylidene fluoride membrane, the membrane was blocked in 5% skim milk at room temperature for 1.2 h and then incubated overnight at 4°C with the antibody. Antibodies against NF-κB, IKKβ, A20, and β-actin were obtained from Abcam (Cambridge, UK). Proteins were visualized with enhanced chemiluminescence. The relative intensity was measured using Quantity One 4.6.2 software (Bio-Rad Laboratories, Hercules, CA, USA) and β-actin was used as an internal control. Data are presented as the mean ± standard deviation (SD) of the percentage of the control intensity.

Statistical analysis

All experimental data were analyzed using SPSS 19.0 statistical software. The data are presented as the mean ± SD, and $P < 0.05$ was considered statistically significant. Analysis of variance was performed to compare data between groups, and the least significant difference t-test was used to compare the groups.

Results

Identification of rat astrocytes by immunofluorescence staining

A rabbit anti-GFAP polyclonal antibody was used for immunofluorescence staining, which showed that the expression of GFAP in cultured astrocytes was localized to the cytoplasm. In cultured rat astrocytes, GFAP was located in the cytoplasm. To determine the positive cell rate ([number of positive cells/total cell number] × 100%), five fields per slice were examined, and the number of positive cells and the total number of cells were counted; the positive rate was calculated to be more than 90% (Fig. 1).

Luciferase assay for miR-136-5p targeting of the IKKβ and A20 genes

To detect miR-136-5p-mediated targeted regulation of the IKKβ and A20 genes, we cloned the 3'UTR sequences of the IKKβ and A20 genes for luciferase detection. Compared with that of the SCI+LV-ctrl group, luciferase activity was significantly activated in the presence of the 3'UTR region from the IKKβ gene after incubation with miR-136-5p ($P < 0.05$). However, luciferase activity was significantly inhibited in the presence of the 3'UTR region from the A20 gene ($P < 0.05$). These results suggest that miR-136-5p may directly act on the 3'UTR regions of the IKKβ and A20 genes and regulate their expression (Fig. 2).

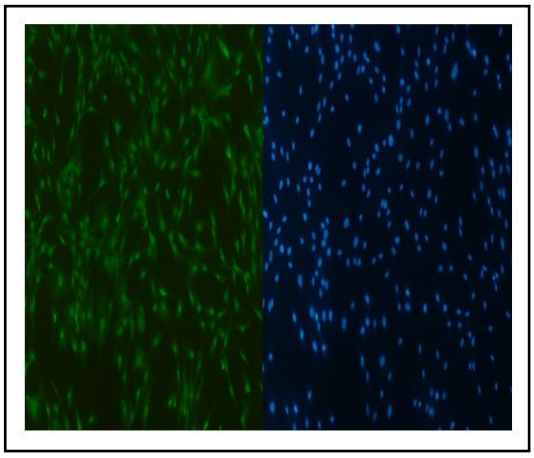

Fig. 1. Immunofluorescence staining of rat astrocytes. (a)x200 Immunofluorescent staining of glial fibrillary acidic protein (GFAP) in rat astrocytes;(b) x200 DAPI staining.

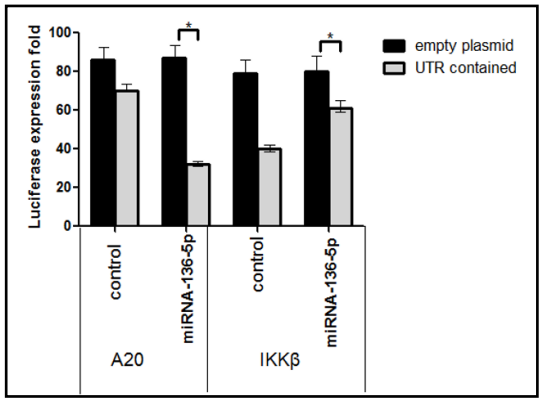

Fig. 2. The plasmid containing the 3'UTR region of A20 gene was significantly down-regulated by miR-136-5p mimics (*p<0.05) and the plasmid containing the 3'UTR region of IKKβ was significantly upregulated by miR-136-5p mimics. Upregulation (*p<0.05)

BBB scores

The rats were placed on a flat surface with dimensions of 2 m × 2 m to observe the movement of the body and limbs after SCI; each rat was observed for 5 min. Behavioral scores were recorded before injury and after the first postoperative day. The results showed no significant difference in preoperative BBB scores ($P > 0.05$) (Table 1). In the SCI model group, the function of both hindlimbs was completely lost, the muscle strength was 0, the rats walked in the prone position, urinary retention was observed, and spinal cord shock appeared. The BBB score was significantly lower in the SCI model group than in the Sham group ($P < 0.05$). The BBB behavioral score immediately after SCI in rats was 0, which indicated a successful operation.

Table 1. Four group rats of average BBB score. Note: *P<0.05, **P<0.01vs NC group

Group	NC	LV-ctrl+SCI	LV-sponge+SCI	LV-miR-136-5p+SCI
Preoperative	20.00±0.0	20.00±0.0	19.8±0.6	20±0.0
First day after operation	19.45±0.6	0.58±0.3**	0.67±0.4**	0.46±0.3**

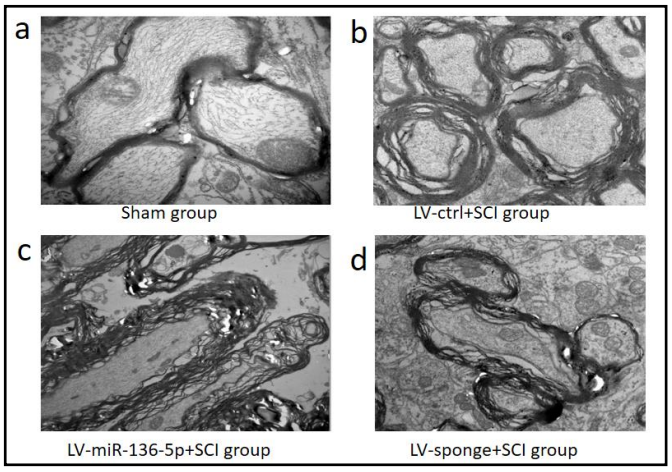

Fig. 3. In the sham group, the myelin sheath was dense and homogeneous (a).After 7 days of SCI, the myelin sheath in the LV-ctrl+SCI group was loosely layeredand the degree of demyelination was lighter (b). The LV-miR-136-5p+SCI group hadmore severe myelin damage(c). Myelin was loosely layered and deprived; whereas inthe LV-sponge+SCI group, myelin damage was significantly reduced compared to theLV-ctrl group had only a slight loose state(d).

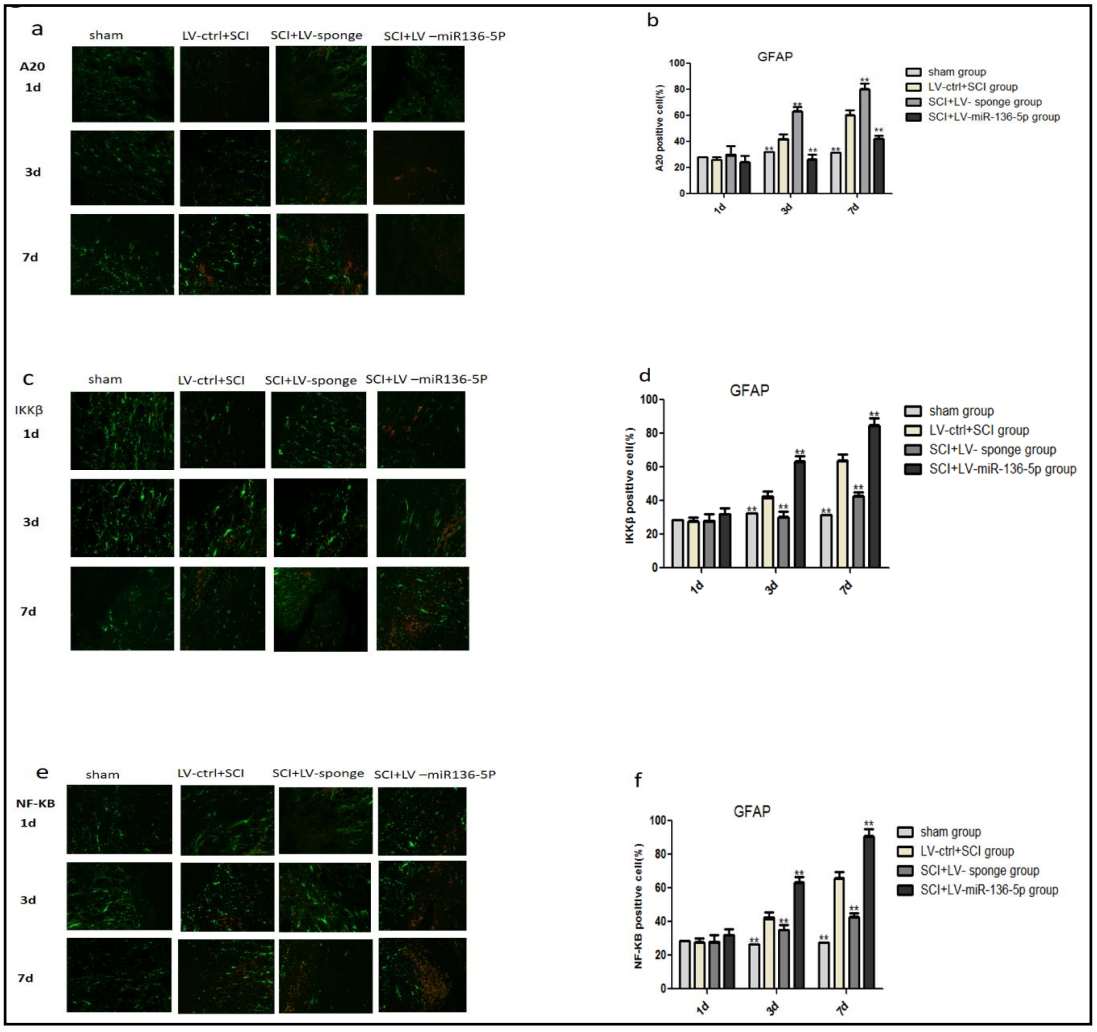

Fig. 4. Double immunofluorescent staining was used to detect the changes of A20(a-b), IKKβ(c-d) and NF-κB (e-f) protein expression in different groups on the 1st, 3rdand 7th day in different experimental groups.

Morphological changes

Transmission electron microscopy was used to observe the changes in the myelin ultrastructure that were induced by LV-miR-136-5p and LV-sponge after SCI in Sprague-Dawley rats. In the Sham group, the myelin sheath was dense and uniform (a). Seven days after SCI, the myelin sheath in the SCI+LV-ctrl group was loosely layered and severely damaged (b). In the SCI+LV-miR136-5p group (c), the myelin sheath injury was severe, and the myelin was loosely stratified and degraded. In contrast, in the SCI+LV-sponge group, the myelin damage was significantly reduced compared with that of the SCI+LV-ctrl group, and the myelin sheath showed only a slightly loose state (d). Thus, the electron microscopy results further confirmed that overexpression of miR-136-5p can indeed increase myelin damage in SCI rats (Fig. 3a–d).

Double immunofluorescence staining

Double immunofluorescence staining (Fig. 4a–f) showed that the infiltration of inflammatory cells into the spinal cord and the expression of p-NF-κB and IKKβ protein was significantly increased in the SCI+LV-ctrl group compared with the Sham group. In contrast, the expression of A20 sharply decreased. Compared with the SCI+LV-ctrl group, the infiltration of inflammatory cells in the miR-136-5p transfected SCI rats was significantly increased and the A20 protein

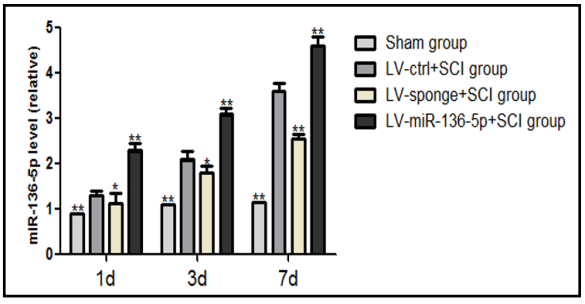

Fig. 5. Expression of miRNA-136-5p in different model groups on the 1st, 3rd and7th day. (* P <0.05, ** p <0.01) vs LV-ctrl+SCI group.

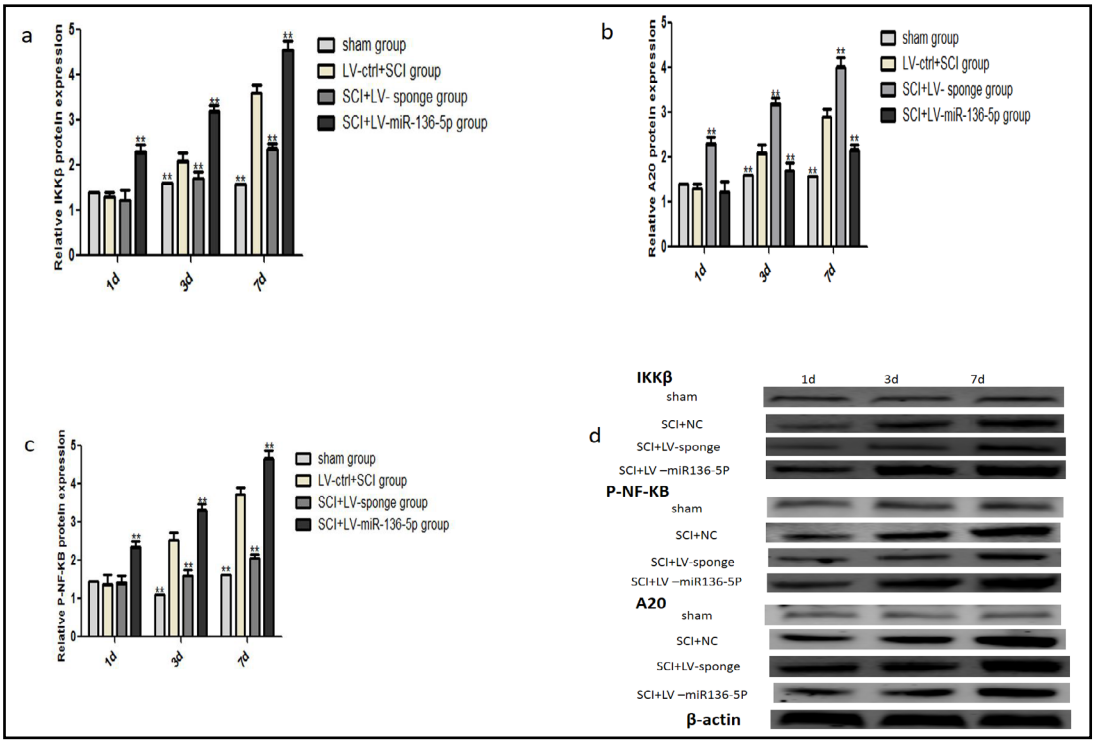

Fig. 6. Western blot analysis of IKKβ, p-NF-κB and A20 (a-d). The effects of miR-136-5p on IKKβ, p-NF-κB and A20 proteins produced by SCI rats. β-actin was used asthe internal control(** p <0.01) vs LV-ctrl+SCI group.

expression in the cytoplasm of spinal glial cells was significantly decreased. In the LV-sponge-infected SCI rats, the infiltration of inflammatory cells and p-NF-κB and IKKβ expression were significantly decreased and A20 expression was significantly increased. These results suggested that miR-136-5p could downregulate the expression of the A20 protein in the spinal cord of SCI rats, upregulate the levels of p-NF-κB and IKKβ, and aggravate the infiltration of inflammatory cells.

Expression pattern of miR-136-5p

The expression of miR-136-5p was measured in the SCI model rats 1, 3, and 7 days after SCI. Compared with the Sham group, the miR-136-5p expression in the SCI+LV-ctrl, SCI+LV-miR136-5p, and SCI+LV-sponge groups began to increase on the first day after SCI, peaking on day 7 after SCI. Compared with the SCI+LV-ctrl group, the miR-136-5p expression was significantly increased in the SCI+LV-miR136-5p group on days 1, 3, and 7 but was lower in the SCI+LV-sponge group. The above results show that miR-136-5p may be upregulated 1 day after SCI. The effect of the transfection of the miR-136-5p construct was clear, and this approach could change the expression level of miR-136-5p in rats (Fig. 5).

Western blotting was used to detect the changes in NF-κB, IKKβ, and A20 protein expression in different groups on days 1, 3, and 7 after the injury. The results showed that the protein expression level of the A20 gene was significantly higher in the SCI+LV-sponge group than in the Sham, SCI+LV-ctrl, and SCI+LV-miR136-5p groups. In addition, the protein expression level was lower in the SCI+LV-miR136-5p group than in the SCI+LV-ctrl group. The expression of the IKKβ and NF-κB proteins in the SCI+LV-miR136-5p group was consistent, with higher levels than in the Sham, SCI+LV-ctrl, and SCI+LV-sponge groups. Furthermore, the protein expression was lower in the SCI+LV-sponge group than in the SCI+LV-ctrl group. At different time points in the same group, there were signs of upregulated protein levels on days 1 and 3 after SCI. Based on the protein expression data, these proteins may accumulate during the SCI-associated inflammatory response (Fig. 6).

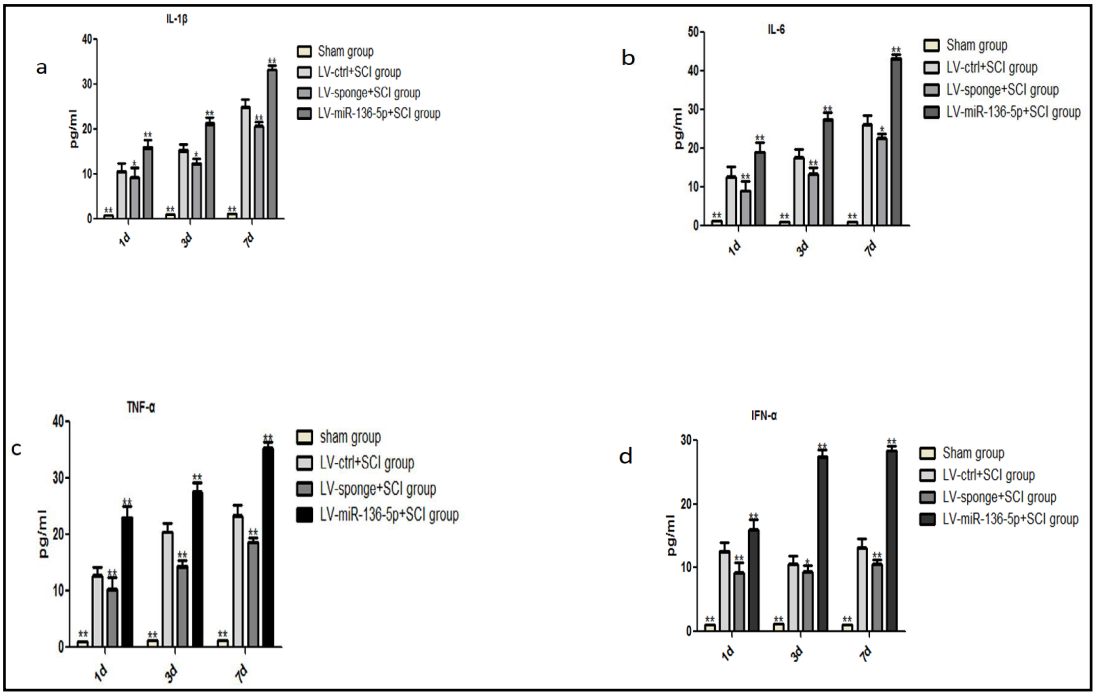

Fig. 7. Enzyme linked immunosorbent assay analysis mainly detected cytokinesinclude IL-1β, IL-6, TNF-α, and IFN-α of the differences in levels of variousinflammatory factors at different time points in different groups (a-d).

ELISA to measure inflammatory factor levels

The IKKβ, NF-κB, and A20 genes are key genes in inflammation-related pathways. ELISA kits were used to detect the levels of inflammatory cytokines at different time points (days 1, 3, and 7) in different experimental groups. Commonly detected cytokines include IL-1β, TNF-α, IL-6, and IFN-α. An analysis of the differences in the levels of various inflammatory factors at different time points in the different groups revealed that on the first day after SCI, the levels of candidate inflammatory factors were significantly higher in the group with SCI than in the Sham group. On day 7, the levels of various inflammatory factors were abnormally high and reached highly significant levels. However, the expression of cytokines was significantly higher in the SCI+LV-miR136-5p group than in the Sham, SCI+LV-ctrl, and SCI+LV-sponge groups. This finding indicates that miRNA 136-5p can significantly increase inflammatory responses in an animal model, suggesting that miR136-5p may play an active role in recovery after SCI by regulating the excessive inflammatory response after SCI through its target genes (IKKβ, A20, and NF-κB) (Fig. 7).

Discussion

An increasing number of studies have found that the immunoinflammatory response after SCI plays an important role in the SCI and the post-injury recovery. Some scholars have confirmed the role of an immunoinflammatory response in SCI and its repair process through animal experiments [26, 27]. In addition, some studies have proposed intervening in the immunoinflammatory response to promote interventions after SCI [28].

According to the time of onset and the direct cause of the disease, SCI is divided into two categories: primary SCI (PSCI) and secondary SCI (SSCI) [29]. PSCI refers to the damage caused directly by external forces during the injury process, including spinal fractures, displacement or dislocation resulting in the compression of bone fragments, SCI, direct axonal disruption, and neuronal and glial cell damage. This process occurs during a short initial period after SCI and these injuries are often irreversible once they occur. At the site of injury, bleeding and ischemia, among other processes, will occur immediately and gradually expand in size, affecting the surrounding normal tissues and triggering the SSCI. The SSCI is based on the PSCI and is caused by hemorrhage and tissue exudate, which continually compress the spinal cord, with roles played by subsequent inflammatory responses and other factors [30]. SSCI gradually produces more proinflammatory factors and chemokines, including IL-6, TNF-α, IFN-γ, and TGF-β. A series of complex damage mechanisms ultimately leads to the demyelination of residual nerve fibers and the degeneration and death of a large number of neurons and glial cells [31]. Because the duration and scope of SSCI extend far beyond those of PSCI, SSCI-associated damage to the spinal cord often far exceeds that of PSCI [32-34].

Of all of the mechanisms of SSCI, immunoinflammatory reactions are one of the most crucial processes. The immunoinflammatory response has two sides. It not only participates in the pathological process of secondary injury, but also plays an important role in the process of injury repair; the equilibration state of the inflammatory response indirectly or directly affects the prognosis of SCI [35]. An increasing number of studies have suggested that immune cells in the brain or spinal cord are the hallmark of a pathological state or impending tissue damage in the body. However, fundamentally speaking, the activation of the immune system is caused by external factors and represents a natural reaction to tissue damage or infection. This process aims to restore the homeostasis in the body or to promote the repair of damaged tissue [36]. Therefore, we believe that immune responses in the nervous system may promote the repair of the central nervous system [37, 38].

After SCI, the immunoinflammatory response, innate immunity, and adaptive immunity alternate throughout the SCI and repair. During the early stage after SCI, a large number of genes related to inflammation are upregulated and gradually return to normal levels. These inflammatory factors include IL-1β, COX-2, IL-6, and TNF-α [39]. However, the use

of cell transplantation, vaccination, or drug treatment to enhance the immune response measures of the central nervous system revealed that the activation of the immune response instead led to a large amount of neuronal and glial cell necrosis. Therefore, the specific mechanism and regulatory process associated with inflammatory responses in the nervous system require further in-depth study to explain the mechanism and clinical value of the immunoinflammatory response after injury to the nervous system.

We found that miR-136-5p, as a modulator of the inflammatory response after SCI, affects immune responses and other types of inflammatory cytokines in the central nervous system. IKKβ/NF-κB/A20 is a common signal transduction pathway. In this study, we determined whether miR-136-5p could upregulate or downregulate the activity of luciferase by selectively regulating the expression of IKKβ/NF-κB/A20. A luciferase assay was used to verify that miR-136-5p could target IKKβ and A20. There is indeed a binding site for miR-136-5p in the 3'UTR sequences of these genes. The expression of miR-136-5p was upregulated after SCI. The expression level of miR-136-5p in the animal model was positively correlated with the levels of inflammatory factors. In this work, a SCI model was established, and lentiviral vectors (LV-ctrl, LV-miR-136-5p, and LV-sponge) were injected into rats. The expression of miR-136-5p in the spinal cord tissue of SCI rats was upregulated after SCI, as indicated by real-time PCR. The upregulated expression level observed after LV-miR-136-5p infection was significant. The serum levels of IL-β, IL-6, IFN-α, and TNF-α were significantly higher in SCI rats infected with LV-miR-136-5p than in the SCI+LV-ctrl group, and the corresponding SCI after LV-sponge treatment was considerable. In rats, the secretion levels of the above inflammatory factors and chemokines were significantly reduced. These findings suggested that miR-136-5p plays an important role in SCI-induced inflammatory reactions.

To further explain this phenomenon, the results of western blotting and immunofluorescence staining showed that the expression of the IKKβ and NF-κB proteins was significantly increased in SCI rats infected with the LV-miR-136-5p virus compared with the LV-sponge rats. After the expression of endogenous miR-136-5p was inhibited, the protein expression levels of IKKβ and NF-κB were significantly reduced. However, the A20 expression results are completely contrary to the results obtained for IKKβ and NF-κB. Taken together, these results suggest that miR-136-5p in SCI rats not only inhibits A20 protein expression, but also upregulates IKKβ and NF-κB expression.

The transmission electron microscopy results showed that myelin was dense in the Sham group but that the myelin sheath was light and loose in the SCI+LV-ctrl group. In the SCI+LV-miR136-5p group, the myelin damage was severe, with a loose myelin layer and myelin loss. The myelin damage in the LV-sponge group was significantly reduced compared with that in the SCI+LV-ctrl group, with only a small amount of the myelin sheath showing a slightly loose state. The above experimental results show that the overexpression of miR-136-5p can aggravate the infiltration of inflammatory cells into the spinal cord in SCI rats; the silencing of miR-136-5p can significantly inhibit the demyelination of the spinal cord that is caused by infiltrating inflammatory cells in SCI rats. Thus, miR-136-5p is involved in the inflammatory response after SCI in the SCI model and has an important influence on the recovery of motor function after SCI. miR-136-5p also provides new strategies and targets for SCI intervention therapy. Due to the longer time period and the experimental difficulty associated with the generation of knockout animals, this study does not exclude the possibility that miR-136-5p regulates other target genes to participate in inflammatory reactions through gene knockout or point mutations. Such investigations would help to better explain the conclusions of this work.

Acknowledgements

This study was supported by the National Natural Science Foundation of China (81560351) and Funded by High Level Innovation Team and Excellence Scholars Program of GuangXi High Education Institutions.

Disclosure Statement

The authors declare no competing financial interests.

References

1 Lam T, Pauhl K, Ferguson A, Malik RN, Krassioukov A, Eng JJ: Training with robot-applied resistance in people with motor-incomplete spinal cord injury: Pilot study. J Rehabil Res Dev 2015;52:113-129.
2 Anwar MA, Al Shehabi TS, Eid AH: Inflammogenesis of secondary spinal cord injury. Front Cell Neurosci 2016;10:98.
3 Ragnarsson KT, Wuermser LA, Cardenas DD, Marino RJ: Spinal cord injury clinical trials for neurologic restoration: Improving care through clinical research. Am J Phys Med Rehabil 2005;84:S77-97; quiz S98-100.
4 Morawietz C, Moffat F: Effects of locomotor training after incomplete spinal cord injury: A systematic review. Arch Phys Med Rehabil 2013;94:2297-2308.
5 Lin L, Lin H, Bai S, Zheng L, Zhang X: Bone marrow mesenchymal stem cells (bmscs) improved functional recovery of spinal cord injury partly by promoting axonal regeneration. Neurochem Int 2018;115:80-84.
6 Profyris C, Cheema SS, Zang D, Azari MF, Boyle K, Petratos S: Degenerative and regenerative mechanisms governing spinal cord injury. Neurobiol Dis 2004;15:415-436.
7 Bareyre FM, Schwab ME: Inflammation, degeneration and regeneration in the injured spinal cord: Insights from DNA microarrays. Trends Neurosci 2003;26:555-563.
8 Aoki E, Yano R, Yokoyama H, Kato H, Araki T: Role of nuclear transcription factor kappa b (nf-kappab) for mptp (1-methyl-4-phenyl-1, 2,3, 6-tetrahyropyridine)-induced apoptosis in nigral neurons of mice. Exp Mol Pathol 2009;86:57-64.
9 Peng X, Shi X, Zhao J, He J, Li K, Cen Z, Wu Y, Zong S, Zeng G: The effects of mir-136-5p-mediated regulation of a20 in astrocytes from cultured spinal cord cultured cells *in vitro*. Cell Physiol Biochem 2017;41:1596-1604.
10 Huang WC, Hung MC: Beyond nf-kappab activation: Nuclear functions of ikappab kinase alpha. J Biomed Sci 2013;20:3.
11 He J, Zhao J, Peng X, Shi X, Zong S, Zeng G: Molecular mechanism of mir-136-5p targeting nf-kappab/a20 in the il-17-mediated inflammatory response after spinal cord injury. Cellular physiology and biochemistry : international journal of experimental cellular physiology, biochemistry, and pharmacology 2017;44:1224-1241.
12 Zong S, Zeng G, Fang Y, Peng J, Tao Y, Li K, Zhao J: The role of il-17 promotes spinal cord neuroinflammation via activation of the transcription factor stat3 after spinal cord injury in the rat. Mediators Inflamm 2014;2014:786947.
13 Ihle JN: Stats: Signal transducers and activators of transcription. Cell 1996;84:331-334.
14 Bulek K, Liu C, Swaidani S, Wang L, Page RC, Gulen MF, Herjan T, Abbadi A, Qian W, Sun D, Lauer M, Hascall V, Misra S, Chance MR, Aronica M, Hamilton T, Li X: The inducible kinase ikki is required for il-17-dependent signaling associated with neutrophilia and pulmonary inflammation. Nat Immunol 2011;12:844-852.
15 Awane M, Andres PG, Li DJ, Reinecker HC: Nf-kappa b-inducing kinase is a common mediator of il-17-, tnf-alpha-, and il-1 beta-induced chemokine promoter activation in intestinal epithelial cells. J Immunol 1999;162:5337-5344.
16 Vereecke L, Beyaert R, van Loo G: The ubiquitin-editing enzyme a20 (tnfaip3) is a central regulator of immunopathology. Trends Immunol 2009;30:383-391.
17 Hymowitz SG, Wertz IE: A20: From ubiquitin editing to tumour suppression. Nat Rev Cancer 2010;10:332-341.
18 Lee EG, Boone DL, Chai S, Libby SL, Chien M, Lodolce JP, Ma A: Failure to regulate tnf-induced nf-kappab and cell death responses in a20-deficient mice. Science 2000;289:2350-2354.
19 Nesic O, Svrakic NM, Xu GY, McAdoo D, Westlund KN, Hulsebosch CE, Ye Z, Galante A, Soteropoulos P, Tolias P, Young W, Hart RP, Perez-Polo JR: DNA microarray analysis of the contused spinal cord: Effect of nmda receptor inhibition. J Neurosci Res 2002;68:406-423.

20 De Biase A, Knoblach SM, Di Giovanni S, Fan C, Molon A, Hoffman EP, Faden AI: Gene expression profiling of experimental traumatic spinal cord injury as a function of distance from impact site and injury severity. Physiol Genomics 2005;22:368-381.
21 Hohjoh H, Fukushima T: Expression profile analysis of microrna (mirna) in mouse central nervous system using a new mirna detection system that examines hybridization signals at every step of washing. Gene 2007;391:39-44.
22 Bak M, Silahtaroglu A, Moller M, Christensen M, Rath MF, Skryabin B, Tommerup N, Kauppinen S: Microrna expression in the adult mouse central nervous system. RNA 2008;14:432-444.
23 Liu G, Detloff MR, Miller KN, Santi L, Houle JD: Exercise modulates microrna that affect the pten/mtor pathway in rats after spinal cord injury. Exp Neurol 2012;233:447-456.
24 McCarthy KD, de Vellis J: Preparation of separate astroglial and oligodendroglial cell cultures from rat cerebral tissue. J Cell Biol 1980;85:890-902.
25 Basso DM, Beattie MS, Bresnahan JC: A sensitive and reliable locomotor rating scale for open field testing in rats. J Neurotrauma 1995;12:1-21.
26 Miljkovic D, Momcilovic M, Stojanovic I, Stosic-Grujicic S, Ramic Z, Mostarica-Stojkovic M: Astrocytes stimulate interleukin-17 and interferon-gamma production *in vitro*. J Neurosci Res 2007;85:3598-3606.
27 Chuah MI, Hale DM, West AK: Interaction of olfactory ensheathing cells with other cell types *in vitro* and after transplantation: Glial scars and inflammation. Exp Neurol 2011;229:46-53.
28 Allison DJ, Ditor DS: Immune dysfunction and chronic inflammation following spinal cord injury. Spinal Cord 2015;53:14-18.
29 Kirshblum SC, Biering-Sorensen F, Betz R, Burns S, Donovan W, Graves DE, Johansen M, Jones L, Mulcahey MJ, Rodriguez GM, Schmidt-Read M, Steeves JD, Tansey K, Waring W: International standards for neurological classification of spinal cord injury: Cases with classification challenges. Top Spinal Cord Inj Rehabil 2014;20:81-89.
30 Correa SG, Maccioni M, Rivero VE, Iribarren P, Sotomayor CE, Riera CM: Cytokines and the immune-neuroendocrine network: What did we learn from infection and autoimmunity? Cytokine Growth Factor Rev 2007;18:125-134.
31 Olivas AD, Noble-Haeusslein LJ: Phospholipase a2 and spinal cord injury: A novel target for therapeutic intervention. Ann Neurol 2006;59:577-579.
32 Park E, Velumian AA, Fehlings MG: The role of excitotoxicity in secondary mechanisms of spinal cord injury: A review with an emphasis on the implications for white matter degeneration. J Neurotrauma 2004;21:754-774.
33 Fehlings MG, Nakashima H, Nagoshi N, Chow DS, Grossman RG, Kopjar B: Rationale, design and critical end points for the riluzole in acute spinal cord injury study (riscis): A randomized, double-blinded, placebo-controlled parallel multi-center trial. Spinal Cord 2016;54:8-15.
34 Zhu H, Poon W, Liu Y, Leung GK, Wong Y, Feng Y, Ng SCP, Tsang KS, Sun DTF, Yeung DK, Shen C, Niu F, Xu Z, Tan P, Tang S, Gao H, Cha Y, So KF, Fleischaker R, Sun D et al.: Phase i-ii clinical trial assessing safety and efficacy of umbilical cord blood mononuclear cell transplant therapy of chronic complete spinal cord injury. Cell Transplant 2016;25:1925-1943.
35 Zhang JX, Hu WW, Liu Z: recent advances in treatment of glial scar-induced inhibition of nerve regeneration. J. Zhejiang Univ.-SCI. B 2009;38:639-643.
36 Oleszak EL, Zaczynska E, Bhattacharjee M, Butunoi C, Legido A, Katsetos CD: Inducible nitric oxide synthase and nitrotyrosine are found in monocytes/macrophages and/or astrocytes in acute, but not in chronic, multiple sclerosis. Clin Diagn Lab Immunol 1998;5:438-445.
37 Schwartz M: Harnessing the immune system for neuroprotection: Therapeutic vaccines for acute and chronic neurodegenerative disorders. Cell Mol Neurobiol 2001;21:617-627.
38 Schwartz M, Kipnis J: Protective autoimmunity: Regulation and prospects for vaccination after brain and spinal cord injuries. Trends Mol Med 2001;7:252-258.
39 Song G, Cechvala C, Resnick DK, Dempsey RJ, Rao VL: Genechip analysis after acute spinal cord injury in rat. J Neurochem 2001;79:804-815.